

**UNDERPLATED UNITS IN AN
ACCRETIONARY COMPLEX: MELANGE OF
THE SHIMANTO BELT OF EASTERN
SHIKOKU, SOUTHWEST JAPAN**

Gaku Kimura and Atsuhiko Mukai

Department of Earth Sciences, Kagawa University,
Takamatsu, Japan

Abstract. Imbricated thrust stacks composed of melange and oceanic slabs occur in the Shimanto Belt, eastern Shikoku, SW Japan. The melanges are divided into two types: Melange I consists of lenticular sandstone blocks surrounded by scaly shale matrix, and Melange II is composed of blocks of oceanic material, such as basalts, cherts and red shale, in a scaly matrix of shale. Melange II is observed only near the boundaries between Melange I and oceanic slabs. The fabric of Melange I indicates progressive deformation during underthrusting of originally coherent trench-fill turbidites. Layer-parallel extension characterizes early deformation and is divided into two stages: an early stage formed during normal faulting, and a subsequent stage formed perpendicular to the early extension. The early extension is interpreted in terms of Riedel shear associated with layer-parallel shearing and tectonically induced loading normal to the layering. The second extension is due to sticking-thrust movement. Late deformation of Melange I is represented by folding in association with layer-parallel shearing. This appears to be related to compression just before or during underplating of Melange I beneath the accretionary prism. Layer-parallel shear extends downward due to strain hardening of sheared sediments and then reaches to

the base of the sediments. Subsequently, the shear zone penetrates pelagic sediments and, finally, oceanic basement. At this time, Melange II is formed by the shearing. An imbricated stack of Melanges I, II and oceanic slabs forms duplexes during the underplating process. The weak metamorphism of the melange complex in the study area suggests that underplating occurs at shallow depths where trench fill is thin.

INTRODUCTION

Studies of modern and ancient accretionary prisms have introduced three types of melange: tectonic melange associated with underthrusting, sedimentary melange due to gravity sliding on the trench slope, and diapiric melange due to intrusion [Cowan, 1985]. Internal fabric of melange is one of the keys to determining the process that contributes to the formation of melange. Although some melanges which show a "block-in-matrix" texture [Raymond, 1984] are characterized by layer-parallel extension during early phases of deformation, seismic reflection profiles at present-day convergent margins indicate folding, imbrication, and other structures reflecting layer-parallel shortening [e.g., McCarthy and Scholl, 1985; Aoki et al., 1982; Lundberg and Moore, 1986]. Thus, layer-extension melanges are considered to result from superficial gravity sliding on the trench slope [Cowan, 1982]. On this basis, many geologists without detailed analysis, considered this kind of melange as an olistostrome. Recent studies, however, have recognized that an

Copyright 1991
by the American Geophysical Union.

Paper number 90TC00799.
0278-7407/90/90TC-00799 \$10.00

underthrust or subducted unit under the decollement is different from an off-scraped one, which is characterized by internal structures due to layer-parallel shortening above the decollement [e.g. Westbrook et al., 1984; Biju Duval et al., 1982].

On the basis of fabric analysis of melange, layer-parallel extension is common within the underthrust unit, which is observed as melange or broken formations [Byrne, 1984; Knipe, 1986; Needham, 1987; Needham and Mackenzie, 1988; Mackenzie et al., 1987; Fisher and Byrne, 1987; Agar, 1988]. Because extension fabric is consistent with layer-parallel shearing, it is emphasized that the layer-parallel extension is characteristic not only of sedimentary melanges caused by superficial gravity sliding with or without subsequent shearing, but also in tectonic melange during initial phases of deformation. Subsequent underthrusting of this unit beneath the decollement can result in underplating at depth or subduction into the mantle. Thus, tectonic melanges have recorded a progressive deformation during underthrusting and underplating [Fisher and Byrne, 1987; Mackenzie et al., 1987]. This process is unlikely in case of sedimentary melange because of its superficial location.

Oceanic materials in melange units are common in the Shimanto Belt. In contrast, underplated bodies in Alaska contain few oceanic sediments [Byrne, 1984; Sample and Fisher, 1986; Fisher and Byrne, 1987]. Melange units with greenstones in the Shimanto of Kyushu [Mackenzie et al., 1987] are thought to have been underplated under greenschist-facies metamorphic conditions. The Shimanto in Kyushu studied by Mackenzie et al. [1987] and Needham and Mackenzie [1988] is exceptional because the region that suffered greenschist-facies metamorphism is limited to a small part of the Shimanto in Japan. On the other hand, the melanges that include oceanic affinities, such as basalts, cherts and limestones without intense metamorphism (weaker than zeolite facies metamorphism), are common in the Shimanto Belt. Thus, the melanges in the Shimanto Belt are useful for studying the progressive underplating of oceanic materials from shallow to deep levels. We have studied the melange of the Shimanto Belt in the eastern part of Shikoku, SW Japan. We describe the detailed process of early extension of coherent layers related to layer-parallel shearing, mixing with oceanic sediments with basement basalts, and the stacking of these units, probably during underplating.

OUTLINE OF STUDY AREA

The Shimanto Belt is situated along the southern coast of western Japan (Figure 1) and is composed of

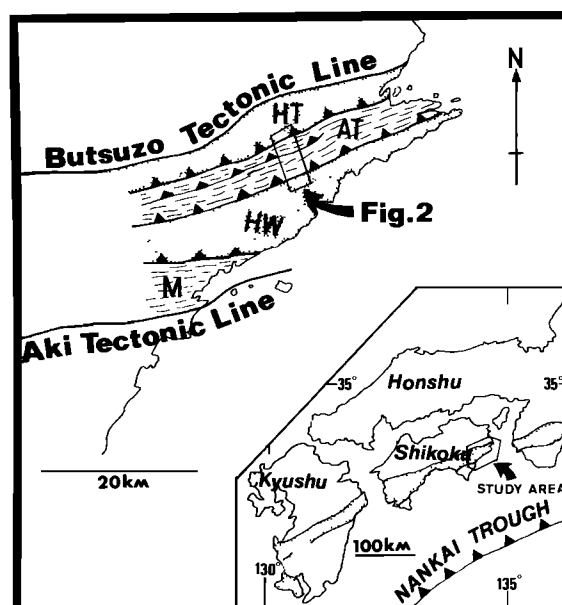


Fig. 1. Index map showing the study area. Dotted area indicates coherent units composed of turbidites and terrigenous sediments. Short dashed line area represents melange units. HT, Hinotani unit; AT, Akamatsu-Taniyama unit; HW, Hiwasa unit; M, Mugi unit. The dotted belt of SW Japan in the right bottom index map shows the Cretaceous Shimanto Belt.

two subbelts: northern Cretaceous and southern Tertiary. The formations in both subbelts consist of coherent turbidite units, broken formations, and melanges. These have been thought to be ancient accretionary complexes [Sakai and Kammerer, 1981; Taira et al., 1980, Ogawa et al., 1988]. There are several opinions about the origin of the Shimanto accretionary complexes, especially of melange. Taira et al. [1980] first revealed an age-lithofacies relationship using radiolarian fossils and suggested a sedimentary process of mixing between the older oceanic material such as ribbon cherts, limestones, and basalts, and younger terrigenous flysch sediments deposited in a slope basin or trench. Alternatively, Mackenzie et al. [1987], Needham [1987] and Needham and Mackenzie [1988] suggested a tectonic process beneath the decollement for melange formation on the basis of a study of the fabric of melange in the Cretaceous Shimanto Belt of Kyushu. Recently, Taira et al. [1988] agreed with tectonic origin beneath the decollement for melange formation. Pickering et al. [1988] suggested a diapiric process for the mixing of exotic materials with terrigenous sediments. These three hypotheses are the same as the mechanisms for the formation of melange in an accretionary complex generally proposed by Cowan [1985].

The Cretaceous Shimanto Belt is bounded by the Butsuzo and the Aki Tectonic Lines at its northern and southern margins, respectively (Figure 1). The Belt is subdivided into four units in the eastern area of Shikoku island: Hinotani, Akamatsu-Taniyama, Hiwasa, and Mugi units from north to south. Each unit is in fault contact with others along northward dipping high-angle reverse faults, although some authors interpreted conformable relationships among them [e. g. Kumon, 1983]. Both the Hinotani and Hiwasa units are composed of coherent turbidites; in contrast, the Akamatsu-Taniyama and Mugi units comprise melange that includes such oceanic material as basalt, cherts and limestones. The Hinotani unit is regarded as an early Cretaceous accretionary prism and overlying slope sediments without melange [Matsugi et al., 1987]. The Akamatsu-Taniyama unit consists of Valanginian to Cenomanian cherts and hemipelagic red shale, and Coniacian to Santonian terrigenous sediments which are mixed up and make melange. Kumon [1983] suggested that the melange of the Akamatsu Taniyama unit is an olistostrome that was formed as a result of collapse of seamounts near the trench and their sedimentary mixing with terrigenous slope or trench fill sediments. He also considered that the Hinotani unit overlies conformably the Akamatsu-Taniyama unit. The age relationship between terrigenous sediments of the Hinotani and Akamatsu-Taniyama units mismatches with

Kumon's model, because micropaleontological study suggests the Hinotani unit is older than the Akamatsu-Taniyama [Matsugi et al., 1987]. As shown later, the boundary between the Hinotani and Akamatsu-Taniyama units is a high angle reverse fault.

The Hiwasa unit comprises conglomerates, massive sandstones, and alternating beds of sandstone and mudstone. They are folded and faulted at a map scale but not intensively broken in outcrop. These strata are considered to have been deposited as trench fill or slope sediments [Taira et al., 1980; Taira, 1985]. The Mugi unit is composed of melange including exotic slabs such as basalts, cherts, and hemipelagic red shales. The exotic slabs are in fault contact with surrounding melange matrix consisting of terrigenous sediments. The age of terrigenous sediments in the Mugi unit is Campanian to Maastrichtian and that of cherts is Albian to Cenomanian [Suyari, 1986]. The contact between the Hiwasa and Mugi units is a northward dipping reverse fault. There is a very clear shear zone between them.

The study area is situated in the Akamatsu-Taniyama unit and along the Akamatsu River (Figure 2). The northern margin of the study area is the boundary between the Hinotani and Akamatsu-Taniyama units. The Akamatsu River runs almost perpendicular to the general trend of this unit, which is represented by foliation in the melange. Outcrops

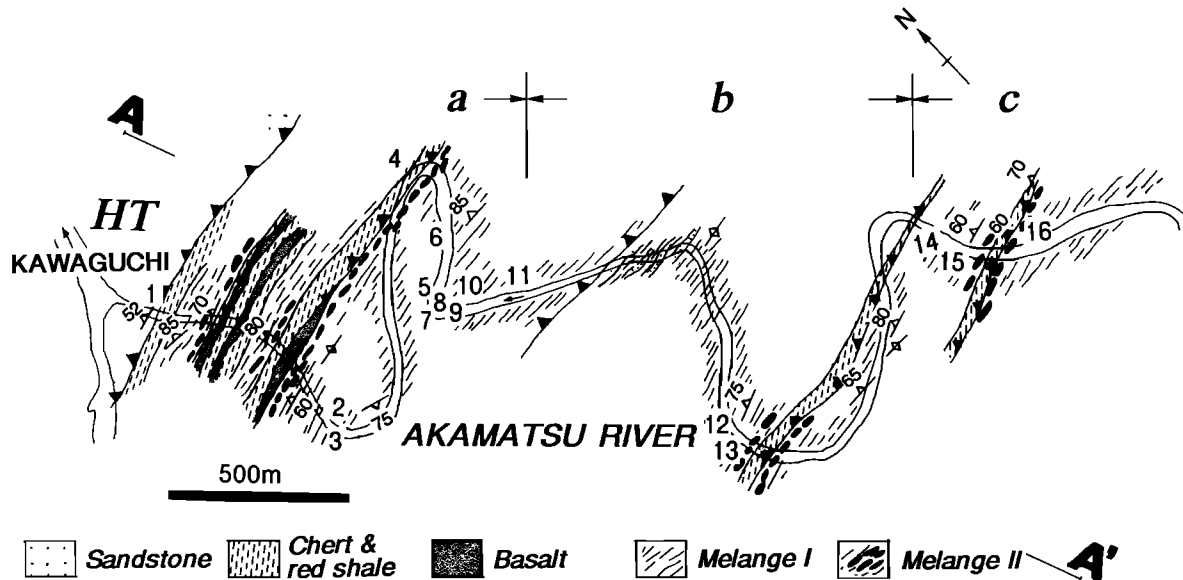


Fig. 2. Sample sites along the Akamatsu River. The oceanic slabs composed of cherts, red shales and basalts alternate with melange. Melange I is composed of lenticular sandstone blocks surrounded by scaly shales. Melange II contains blocks of

oceanic affinities such as cherts and basalts in scaly shale matrix. HT, Hinotani unit; A-A', profiling line of Figure 3 a,b, and c, the areas where veins are measured.

in this river are suitable to observe the melange. Foliations in the melange mostly strike ENE and dip northward steeply.

MELANGE IN THE AKAMATSU RIVER

Along the Akamatsu River, melanges well crop out well (Figure 3). The term melange in the Shimanto Belt has been used where lithofacies show a block-in-matrix character and where their blocks are exotic (for example, such oceanic affinities as cherts and greenstones surrounded by terrigenous sediment matrix) [Taira et al., 1980]. In the Akamatsu River, however, this kind of rock unit is limited; most rocks show block in matrix fabric and suggest originally coherent alternating layers of sandstones and mudstones. Raymond [1984] has defined such a lithofacies as one type of the melanges. We use Raymond's definition in this paper.

At the northern margin of the study area, thick sandstone layers of the Hinotani unit crop out. They are in contact with melange of the Akamatsu-Taniyama unit along a reverse fault dipping northward at about 70° (Figure 3). Three different kinds of lithofacies are observed along the Akamatsu River. The first, the most common type, is characterized by boudinaged blocks of sandstones in a matrix of scaly shales in outcrop scale (we call these Melange I in this paper, Figures 2 and 3). There are matrix-dominant and block dominant parts (Figure 3). The second lithofacies is chert, red shale and pillow basalt bodies with minor limestones. They do not include terrigenous

sediment at all, and are bounded by high-angle reverse faults with Melange I. They are probably platy slabs because they and Melange I occur alternatively. In addition, these bodies continue for several hundred meters to several kilometers parallel to the general foliation of melange (Figure 3). Where both basalts and cherts are observed, the basalts occur exclusively in the southern part of the slab. This means that the slabs of oceanic affinities face northward, if basalts and cherts are the oceanic basement and sedimentary blanket covering them, respectively.

The third occurrence is blocks of oceanic affinities in a matrix of terrigenous sediments in an outcrop scale. They occur only near the boundary between the slab of oceanic materials and Melange I (Figure 3). We call this occurrence of melange as Melange II. Many radiolarian fossils have been reported from the cherts in the Akamatsu River and their extension [Kumon, 1983; Suyari, 1986]. Five slabs of cherts in the Akamatsu River show almost the same age interval from Valanginian to Cenomanian. As the repetition of oceanic units in terms of reverse faults is clear, the deeper part of the profile along the Akamatsu River is considered as in Figure 3. The depth of any major fault or decollement is speculative because of no information at depth.

CHARACTERISTICS OF MELANGE

The dominant melange, containing blocks of sandstones in shale matrix (Melange I), represents three different kinds of structures which appear to coincide with deformation stages. The first type of

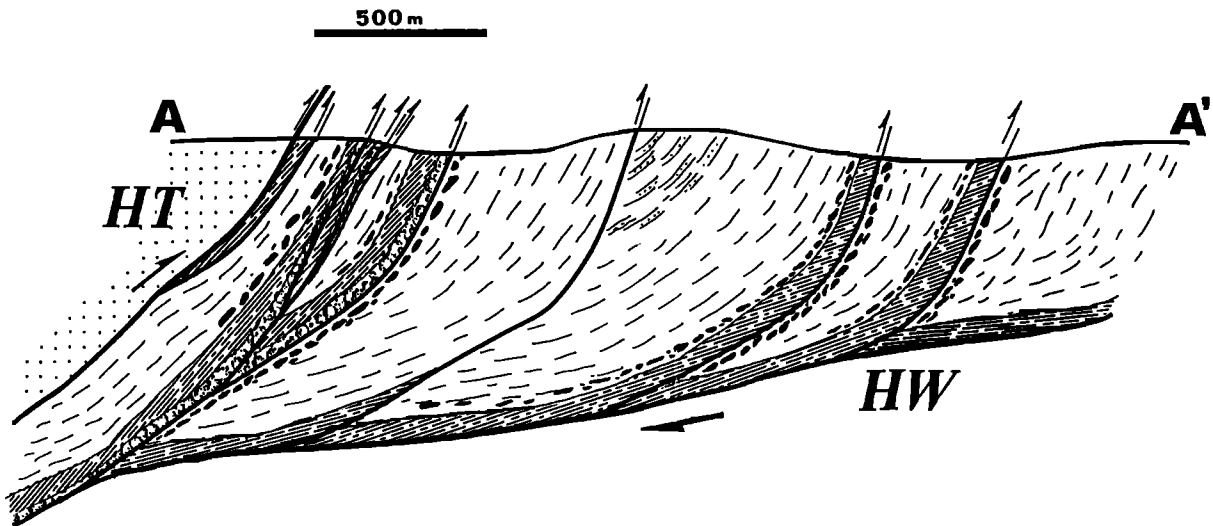


Fig. 3. A geologic profile along the route of the Akamatsu river. Depth of decollement is speculative because of the lack of information at depth. HT,

Hinotani unit composed of coherent turbidites. HW, a coherent unit of Hiwasa unit. The legends showing lithofacies are the same as those of Figure 2.

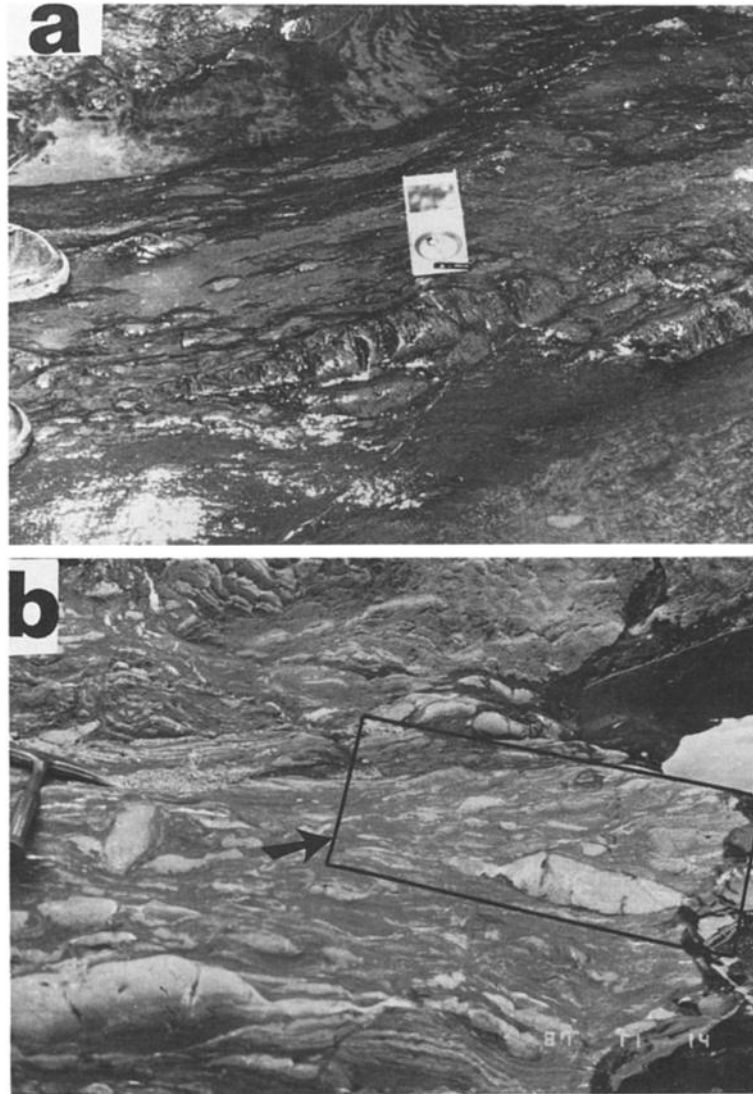


Fig. 4. Two types of occurrence of sandstone blocks in scaly shale matrix. (a) Boudinage structure showing necking due to calcite veins filling extension

fractures. (b) Boudins necked by normal faulting. The box with an arrow corresponds to the area of Figure 5a.

structure is pinch and swell and boudinage, necked perpendicular to the layer (Figures 4a and 5b). Calcite or quartz veins are developed very densely around the pinched region between the swell or tails of boudinaged blocks of sandstones. The second type of structure is shown in Figures. 4b and 5a. Blocks are cut and displaced by normal faults which are oblique to the layering at low angles. The normal faults separate sandstone layers into many blocks. Many cataclastic networks of faults (web structure) are also developed, not only around the necks or tails but in all parts of the lenses (Figure 4b). Both the

two types cited above resulted from layer-parallel extension. The third type of structure is a folded pinch-and-swell structure. This type is rare in the melange of the Akamatsu River. It is illustrated in Figure 6b and 6d. A necked sandstone is folded at its pinched region. Web structures are also developed within the sandstone. An asymmetric fold shows the sense of shear along the foliation. The sense of shear deduced from the fold indicates an uplifting of the northern block, which is consistent with the sense that was inferred from an asymmetric flow structure in the matrix adjacent to the folded boudins (Figures

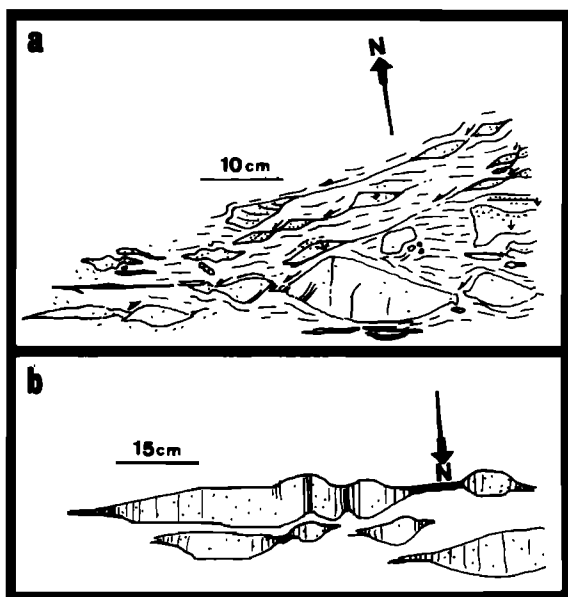


Fig. 5. Sketches showing two kinds of occurrence of boudinage structures. (a) Boudinage structure necked by normal faults from Figure 4b. (b) Boudinage structures whose necks are filled by calcite or quartz veins perpendicular to the layering (from Figure 4a).

6a and 6c). The third example shows compression in association with layer-parallel shear occurring later than layer-parallel extension.

Deformation chronology appears to be: first, normal faulting under the semi-consolidated conditions; second, veining developed in the consolidated sediments, and finally, folding.

Orientations of Veins and Normal Faults

As mentioned above, veins and normal faults recognized within the lenticular sandstone blocks are intimately related to pinch and swell, and boudinage formation. We measured the orientations of these fractures along the Akamatsu River. Figures 7 and 8 represents the orientations of veins and normal faults, respectively. The normal faults are rather small in number. Two orientations were recognized in the veins. In one, the veins trend NNW-SSE and dip almost vertical. In the second, the veins trend ENE-WSW and dip vertical. The former is more common than the latter. The orientation of the former veins is perpendicular to the foliation and strike of melange while that of the latter is parallel to the foliations of melange. Horizontal veins perpendicular to both the foliation and shear

direction are rare. The orientation of the normal faults (Figure 8) is a little different from that of veins. Dominant orientation is E-W strike with steep dip, which is slightly oblique to the foliation of the melange matrix. On the outcrops, the normal faults are not regarded as true normal faults but reverse faults on the present profiles because of mostly vertical foliations of melange. Most of the normal faults appear to have been developed when the sediments were semi-consolidated, and bedding was still horizontal, because they show both deformation mechanisms, grain boundary sliding and cataclastic breakage of the grains (Figure 13). As the normal faults are interpreted to have been formed in an early stage of deformation before complete consolidation of the sediments, the foliations of the melange, which appear to be parallel to original bedding of coherent layers, are corrected to original horizontal situation. After the bedding correction, the visual reverse faults are corrected to normal faults.

Three-Dimensional Features of Lenticular Sandstone Blocks

In an outcrop, we observe mostly two dimensional profiles of sandstone blocks on any surface. As the lenticular blocks are mostly separated from each other, ellipsoidal shape is expected. The shortest axis of the lens is apparently normal to the foliation of melange. Which orientation is the longest axis of the lens is unclear in the Shimanto Belt with the exception of northern Kyushu, where N-S trending long axes parallel to the shear direction of the melange are dominant [Needham and Mackenzie, 1988]. As it is not easy to measure three axes of individual lenticular blocks because of the difficulty of lifting them from the outcrop, we have used the following method to record the ratio among the three axes. Since the shortest axis is always normal to the foliation, we have to choose outcrop surfaces perpendicular to the foliation and including the longest or intermediate axes. As stated in the previous section, veins and normal faults contribute to the formation of boudinage of the sandstone layers. The first boudinage took place by normal faulting with E-W strike. It resulted in N-S trending layer-parallel extension. The second necking dominantly occurred in association with WNW trending vein formations indicating ENE layer-parallel extension. As the strikes of normal faults and dominant veins are almost perpendicular to each other, it appears that the longest and intermediate axes of lenticular sandstone coincide with the strike of veins or normal faults and are parallel to the foliation. We examined the relationship between

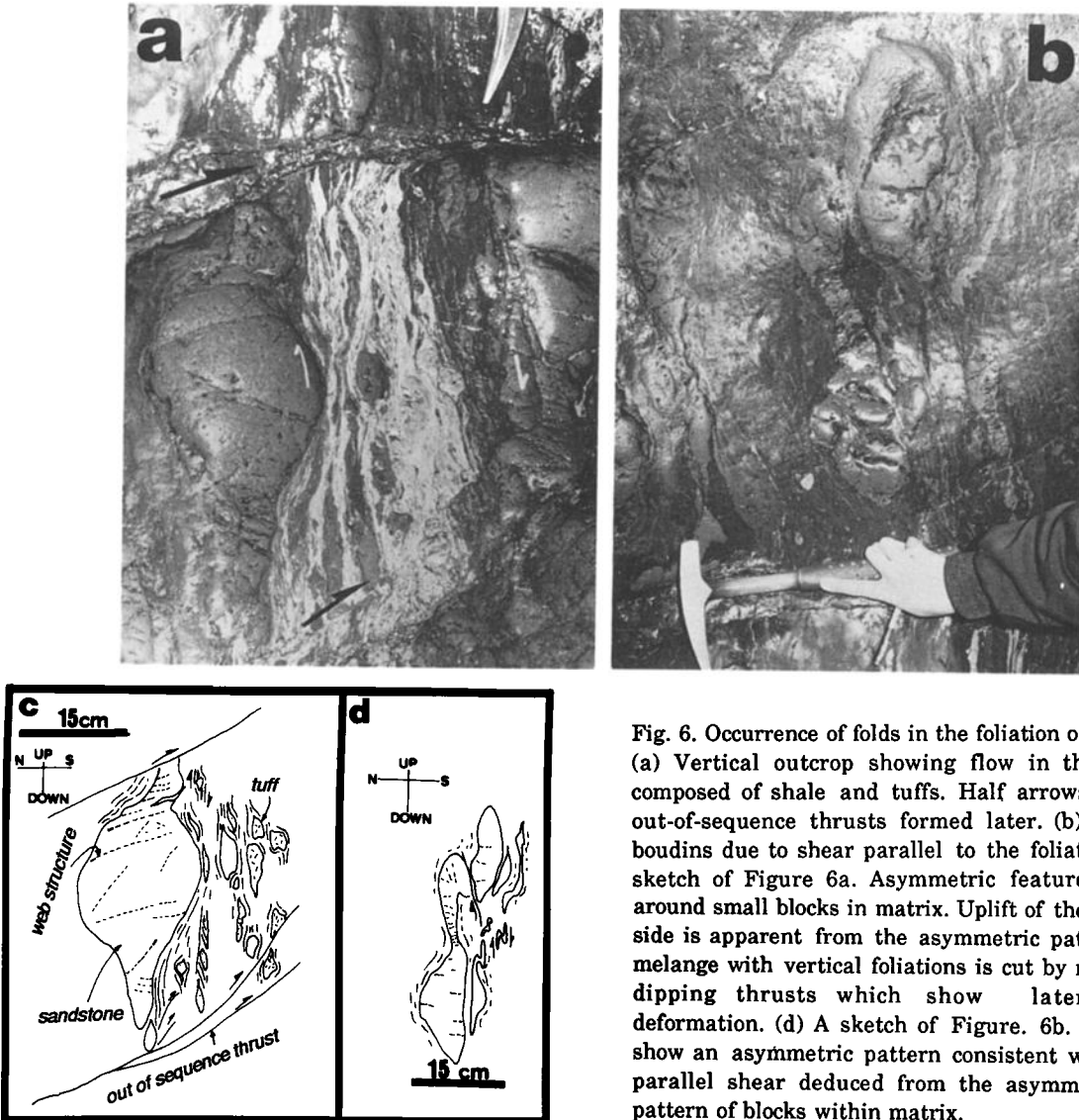


Fig. 6. Occurrence of folds in the foliation of melange. (a) Vertical outcrop showing flow in the matrix composed of shale and tuffs. Half arrows indicate out-of-sequence thrusts formed later. (b) Refolded boudins due to shear parallel to the foliation. (c) A sketch of Figure 6a. Asymmetric feature is clear around small blocks in matrix. Uplift of the northern side is apparent from the asymmetric pattern. The melange with vertical foliations is cut by northward dipping thrusts which show later brittle deformation. (d) A sketch of Figure 6b. The folds show an asymmetric pattern consistent with layer-parallel shear deduced from the asymmetric flow pattern of blocks within matrix.

these three axes, fractures of veins and normal faults within the lenses, and obtained a good agreement between the orientations of fractures and axes of ellipsoidal sandstone lenses. We know empirically that as the length of the longer axis of the lens on the profile increases, the length of the shorter axis also increases, while the ratio between the two axes is almost constant [Uemura, 1965].

With the background mentioned above, we measured the shape of lenses as follows (Figure 9). (1) We chose two outcrop surfaces. One of them is perpendicular to the foliation and parallel to the veins and another one is perpendicular to the foliation and above cited surface. (2) We measured the length of the longest and shortest axes of lenses

on each surfaces. There are several tens of samples on one surface. (3) We estimated the average ratio between the longest and shortest axes on one surface using the minimum square method. We obtained two ratios on the two surfaces. (4) As the shortest axis on both surfaces coincides, the ratio among longest, intermediate, and shortest axes in three dimension is available in comparison with two ratios.

Figure 10 shows individual data. An average ratio between the axes surface is represented by the tangent of the line. We have obtained sixteen averaged ratios in the study area (Figures 10 and 11). The ratios between the longest (a) and intermediate (b) axes are from 1 to 2.5 and mostly less than 2. The ratios between the intermediate (b)

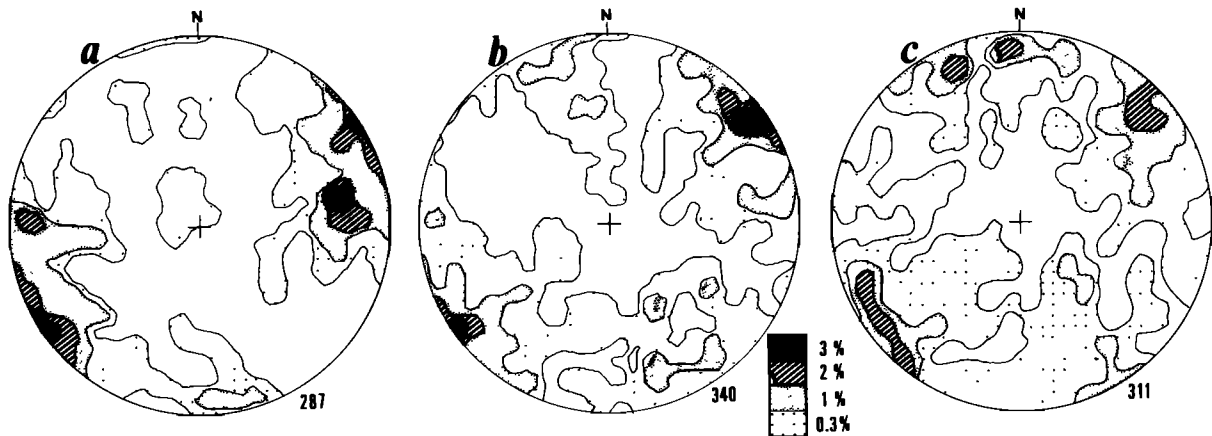


Fig. 7. Equal area projections (lower hemisphere) of poles to veins within the sandstone blocks surrounded by scaly shale matrix in the melange. (a), (b), and (c) show areas where veins are measured in

Figure 2. NNW trending veins are dominant. They are almost perpendicular to the strike of foliations of melange. The secondary dominant orientations are ENE parallel to the strike of the melange.

and shortest (c) axes vary from about 2 to 4.5. Two thirds of the data show a "oblate" type of ellipsoid with the E-W trending longest axis mostly parallel to the strike of melange and a vertical intermediate axis that coincides with the shear direction. This shape of lens is very similar to those reported from the Kodiak Island, Alaska [Byrne, 1984; Fisher and Byrne, 1987] but different from those in the Franciscan of California [Cowan, 1982; Aalto, 1981] and the Shimanto in Kyushu [Needham and Mackenzie, 1988].

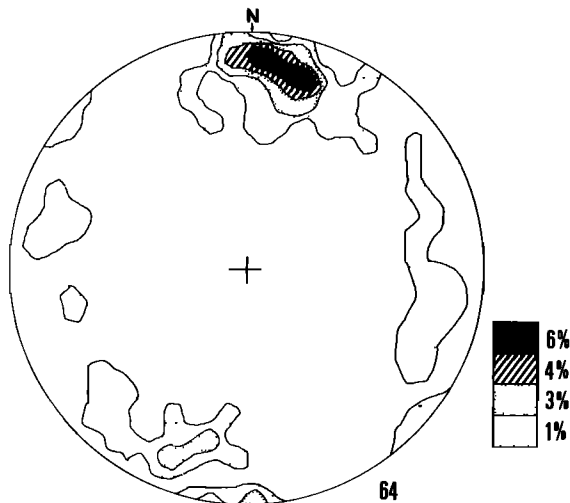


Fig. 8. Equal area projection (lower hemisphere) of poles showing orientations of minor normal faults cutting sandstone blocks in the melange. E-W trending fault predominate.

Microscopic Observation of Lenticular Sandstones

We observed internal structures of the boudinaged sandstone using a polarizing microscope. Under the microscope, there are two kinds of boudinaged sandstones: necking in association with veining or normal faulting (Figures 12 and 13). These are similar to the structures in outcrop scale. Grain size of sandstone in the neck is smaller than elsewhere in the lens. It appears to result from the breakage of grains. Figure 12a shows larger grains floating in the finer matrix around the neck, while no breakage of grains is observed in the central part of the boudinaged sandstone. Disaggregation is clear in the margin of the lens (block arrow in Figure 12a). Fish-like texture due to displacement along the normal faults is common on the section facing eastward or westward (Figure 13). These normal faults are oblique to foliation in the parts where sandstone layers are cut by the faults, but the faults apart from the sandstone blocks change their angle and converge to the foliation in the matrix. The shear gouges show grain boundary sliding. In some case, the gouges of the normal faults are filled by calcite veins (Figure 12b arrow). Deformation structures earlier than the normal faults or veins are characterized by particulate flow which is sometime observed in sandstones dikes.

Deformation of Matrix Shale

Scaly cleavages are pervasively developed in the matrix shale. The cleavages are shear planes themselves, along which there were small displacements. Under the microscope, several grades

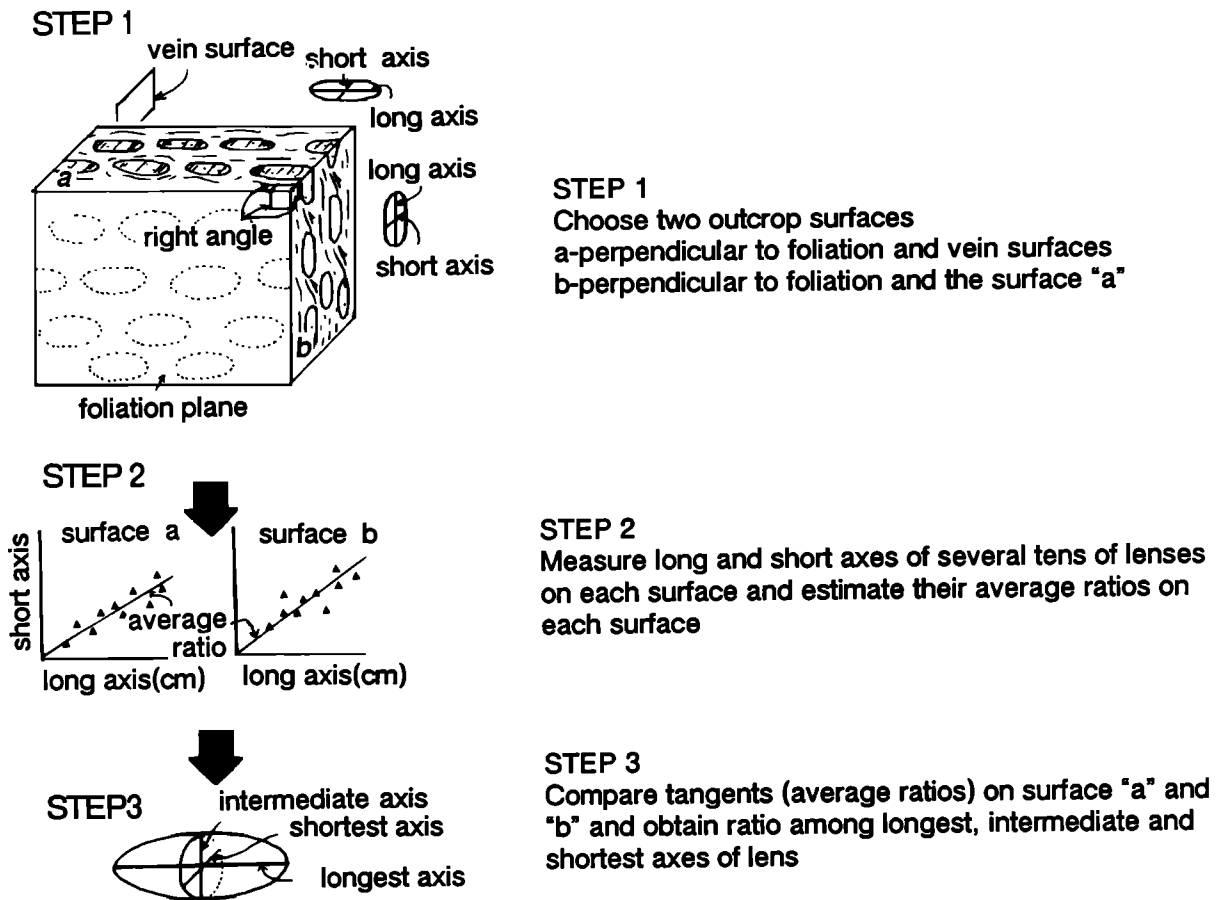
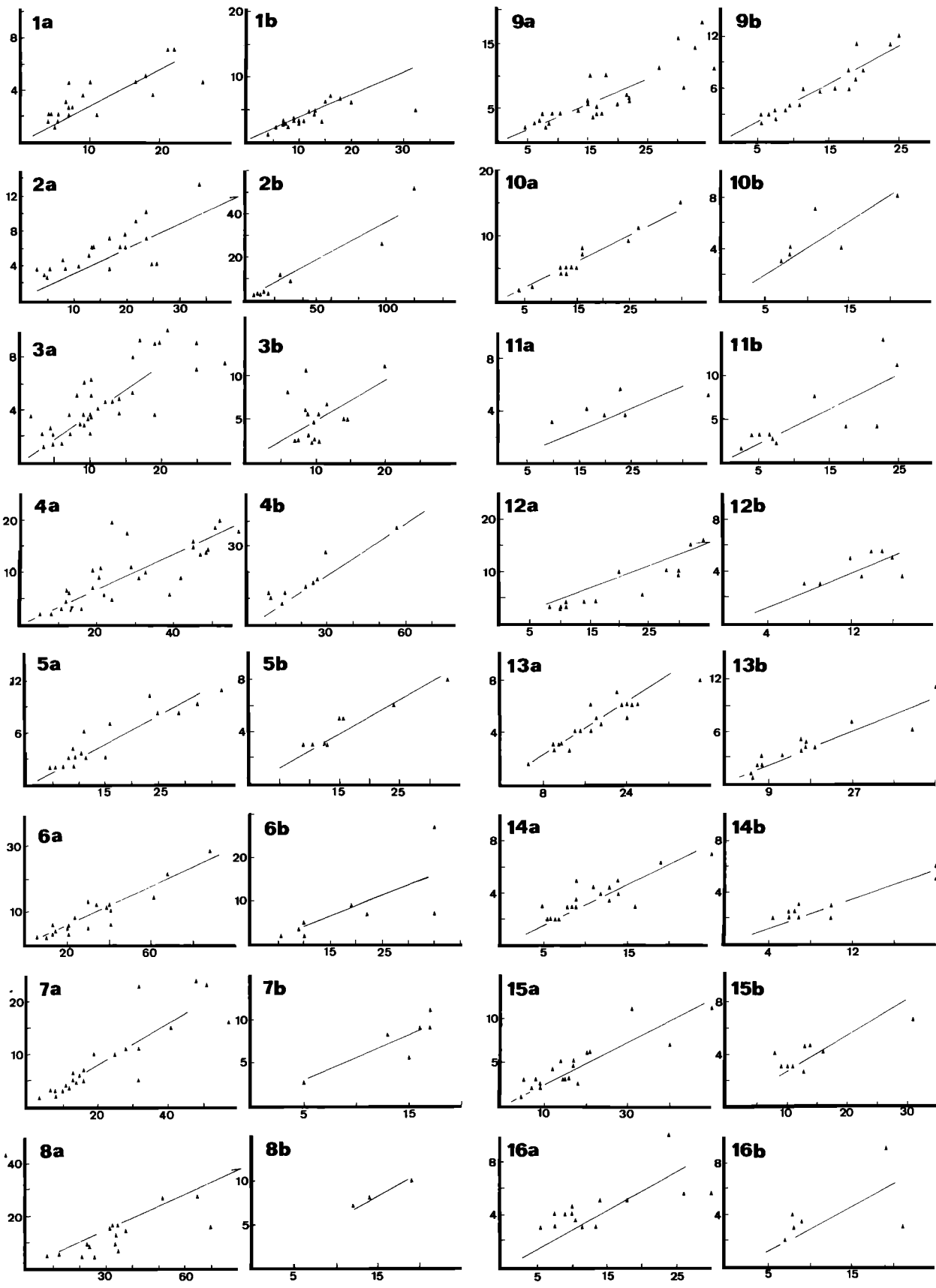


Fig. 9. Data processing flow for analysis of the features of lenticular sandstone blocks in Melange I.

of deformation mode are recognized. Figure 14b indicates rather weak deformation of shale which is represented by limited shear zones and pervasive rearrangement of grains. The shear zones are not continuous but developed in an echelon style (Figure 14b). Fine grains of elongated shape seem to have been rearranged in a style showing the longest axes of minerals parallel to the foliation. A deformed radiolarian is seen in Figures 14b and 14c. It was deformed into an ellipsoidal shape from an original sphere, therefore strain resulted from the deformation and can be estimated from the shape. The longest axis of the deformed radiolaria is oblique to the foliation, suggesting shearing along the foliation. The more deformed shale is shown in Figure 14a. Foliations regarded as scaly cleavages are developed pervasively in the shale. Two orientations of major and secondary foliations, are commonly observed. The major foliation has a thicker gouge zone than the secondary one; for example, in the bottom of Figure 14a. The major one

is consistent with the general trend of melange. The secondary foliation is oblique, but curves and merges into the major foliation. The acute angle between the major and secondary foliations faces toward the south when the major foliation is corrected to the horizontal plane. This oblique sense is the same as that of the normal faults seen in the sandstone lenses. This pattern of scaly cleavage or foliations is consistent with the sense of shear inferred from the deformed radiolaria tests mentioned above. The foliation surfaces show dark seams, tens to several hundred microns in thickness (Figures 14a, 14b, and 14c). These different grades of deformation in the shale suggest a progressive deformation mechanism of the scaly shale. First, shale is deformed due to rearrangement of each grains (grain boundary sliding) and limited shear planes are developed. Before much displacement accumulates along the planes, the previous planes are abandoned and the other shear planes are created. Shear zones having two orientations are generated in the shale.



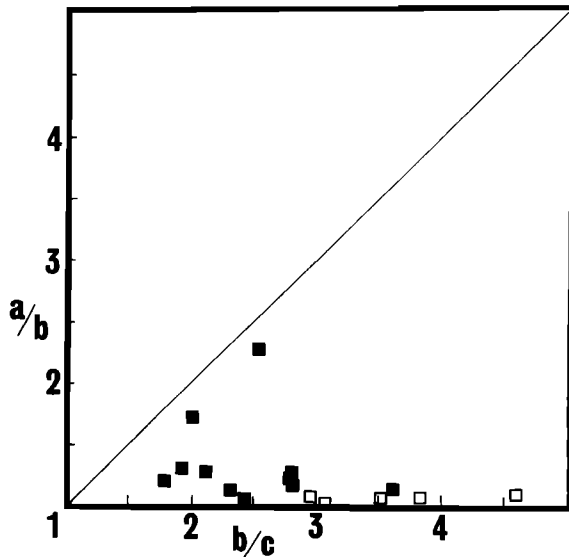


Fig. 11. An X-Y plot showing the feature of ellipsoidal sandstone blocks in the melange. $a:b:c$ is a ratio of longest, intermediate, and the shortest axes of ellipsoid. A solid square indicates ellipsoidal block with horizontal, E-W trending "a" axis, whereas, a open square represents a block with almost N-S trending "a" axis parallel to the foliation.

Strain of the Shale

As stated in the previous section, deformed radiolaria tests are found in the scaly shale. They are very useful to determine strain in the shale. We have measured the ratio of the three axes of the deformed radiolaria tests using microphotographs taken from two orientations of thin sections, one of which is parallel to NNW trending shear direction and perpendicular to the foliation, and another of which is perpendicular to the foliation and shear direction. The shear direction is known from striations on the foliation surface. The results are shown in Figure 15. An average line calculated by the minimum square method suggests that an average strain ellipsoid is represented by a ratio of the three axes of about 1:0.85:0.65. The longest axis

is parallel to the shear direction and the intermediate axis is perpendicular. The average value of strain of the scaly shale is mainly from rather weakly deformed shale, because no radiolarian fossils are found from intensively deformed shale. The value calculated above is smaller than those from more deformed cherts in the metamorphic accretionary complex of the Shimanto Belt in Kyushu [Toriumi and Teruya, 1988].

General Mode of Deformation in Melange I

On the basis of the observations of deformation in outcrop and microscopic scales, a generalized deformation feature of Melange I composed of terrigenous materials is synthesized. The sandstone layers are broken through progressive deformation processes. The earliest deformation is characterized by grain boundary sliding or particulate flow which is observed as sandstone dikes in the weakly deformed parts and shows apparently the deformation of unconsolidated sediments. The lenticular sandstones surrounded by scaly shale matrix appear to have been developed through two stages of layer-parallel extension. The first stage extension is represented by normal faults which strike E-W. The sediments may have been semi-consolidated at this time, because both grain boundary sliding and grain breakage due to cataclastic process are observed along the fault surfaces and within the sandstone. The subsequent stage of extension is characterized by veins developed pervasively in the sandstone lenses. The veins were developed by mostly E-W striking extension parallel to the layering and perpendicular to the shear direction. As the deformation features of veins under the microscope indicate brittle failure, the sediments at this stage appear to have been consolidated. The lenticular sandstones that result from two stages of layer-parallel extension are schematically represented in Figure 16. The three-dimensional shapes of sandstone lenses are different from the strained radiolarian fossils in scaly shale. The longest axes of sandstone blocks are oriented parallel to the layer and are almost E-W trending, while radiolarias have long axes trending N-S. The

Fig. 10. Basic data for estimation of three dimensional features of ellipsoidal sandstone blocks in the melange. Graphs annotated by suffix "a" represent data of longer and shorter axes of elliptical sandstone blocks on predominantly horizontal surfaces of outcrop at sites 1 to 16 (Figure 2), whereas graphs annotated by suffix "b" show the

same ratio on predominantly vertical surfaces of outcrops near the surface "a". Both the vertical and horizontal scales are axial length in cm. On the basis of both the ratios, the ratio $a:b:c$, showing the three dimensional features of ellipsoidal sandstone blocks, is obtained. Localities of measurements are shown in Fig. 2.

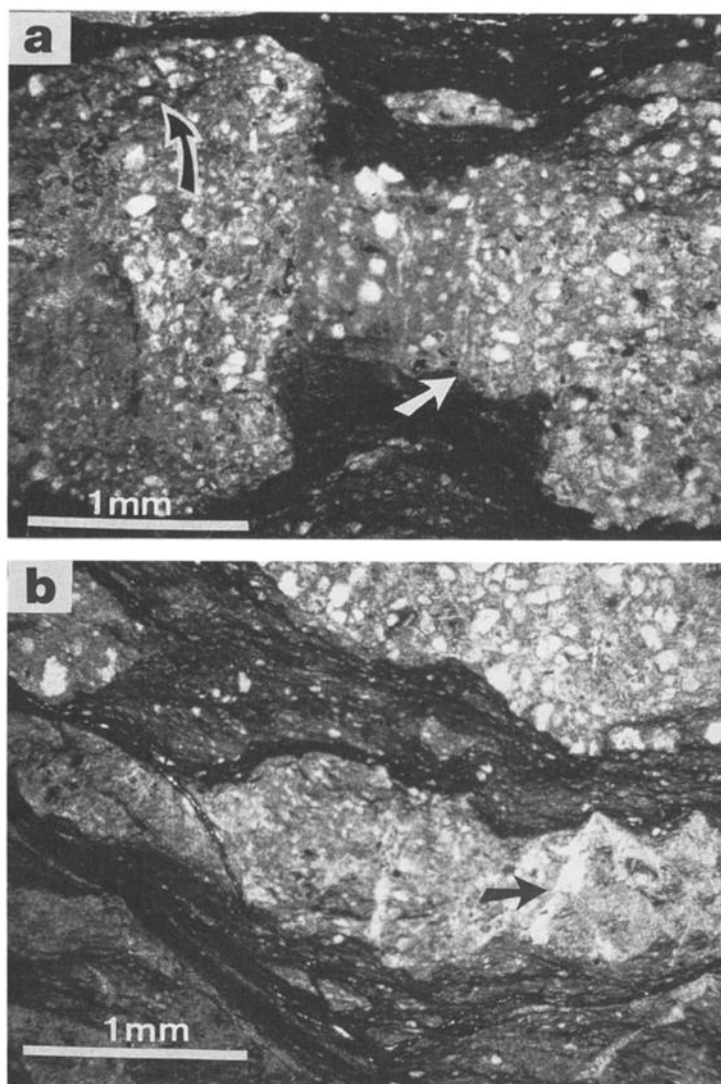


Fig. 12. Texture of necked sandstone blocks in the melange under the microscope. (a) Necking of sandstone due to thinning associated with veins perpendicular to the layering of sandstone. As well as veins, crushed grains are recognized in the neck

region where rather larger grains are floating in the fine crushed matrix. (b) Veins with minor displacement (normal faults). In this case veins are not perpendicular to the long axis of blocks.

ellipsoidal radiolaria are apparently a strain marker, but the sandstone lenses are not.

A more progressive stage of deformation is characterized by folding of boudinaged sandstones.

Features of Melange II at Outcrop Scale

Melange II is characterized by blocks of oceanic affinities such as basalts, cherts, and red shales in scaly shale matrix. Since the oceanic materials did not accumulate at or near the trench but moved

there and were mixed with terrigenous sediments through some process, they are called exotic materials [Taira et al., 1980]. Figure 17 shows an example of the boundary between cherts with red shale and terrigenous black shales. The cherts are folded and sheared by layer-parallel faults. A small-scale duplex structure is recognized in the chert. The sense of shear indicated by the duplex is consistent with that of asymmetric folds formed by drag in association with layer-parallel shear. The bedded cherts alternate with red shales. Near the boundary

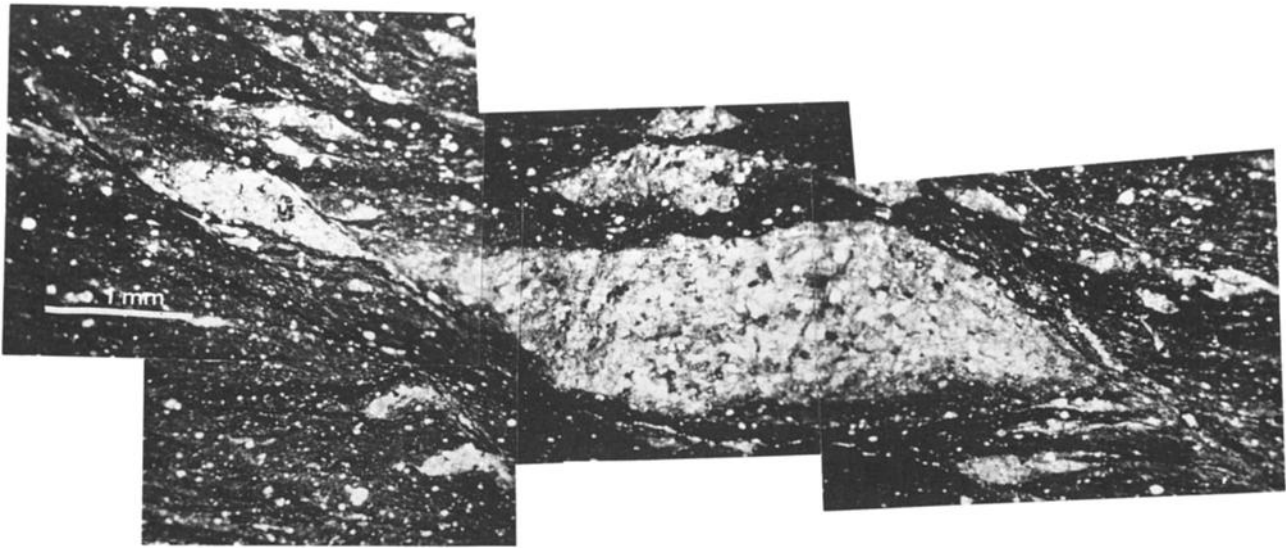


Fig. 13. Rhombic feature of boudinaged sandstone blocks in the melange. Normal faults separating the sandstone blocks merge the foliations of the melange. Veins are also recognized in the lens. Along

the normal faults, disaggregation and grain boundary sliding are observed together with breakage of grains.

between the red shales and black shales, red shales are sheared and scaly cleavages are formed (Figure 17). In the sheared red shale, manganese-rich lenses are recognized as well as lenses of black shale. Black shales near the boundary are also sheared and include, alternatively, lenses of red shales and cherts. Lenses of oceanic material in black shale matrix are recognized only near the boundary between the oceanic slab and terrigenous sediments. Map scale slabs of oceanic affinity alternating with terrigenous shale can be regarded as giant blocks in matrix, but we use "block-in-matrix structure" when they are recognized in outcrop or smaller scale.

Microscopic-Scale Observations

Figures 18a and 18b show microscopic features of Melange II. The breakage of a chert block surrounded by shale matrix is illustrated in Figure 18b. Fractures oblique to the foliation are formed in the chert. The black shale of the matrix injects into the fractures within the fragmented chert. Small domains of chert would be separated by slip along the fractures and make "block-in-matrix" texture in much smaller scale. A more progressive stage of deformation is seen in Figure 18a. Rhombic chert blocks floating in the shale matrix seem to result from the separation of small domains as observed in Figure 18b. The shales of the matrix are deformed similar to the matrix of Melange I. The foliations are

composed mainly of two orientations; the major and secondary ones are oblique to each other and fish-like domains are pervasively developed. The secondary foliations are merged to the major foliation. Both foliations are composed of dark seams consisting mainly of phyllosilicates.

DISCUSSION

Deformation Mechanisms of Melange I

Two stages of extension. Melange I, composed of lenticular sandstone blocks in a matrix of scaly shale, has a systematic fabric as mentioned. The deformation mechanisms of this type of melange have been discussed on the basis of fabric analysis at various scales [Byrne, 1984; Fisher and Byrne, 1987; Knipe, 1986; Needham, 1987; Mackenzie et al., 1987; Needham and Mackenzie, 1988].

Byrne [1984] showed that the orientation of veins is variable in the Ghost Rock melange of Kodiak Island, and Fisher and Byrne [1987] reported that veins perpendicular to the shear direction are dominant. This means that extension parallel to the shear direction prevailed. Layer-parallel extension recorded by normal faults is also parallel to the shear direction in the case of the Kodiak [Fisher and Byrne, 1987] and the Shimanto [Needham, 1987; this study]. Fisher and Byrne [1987] implied that layer-parallel extension in association with layer-

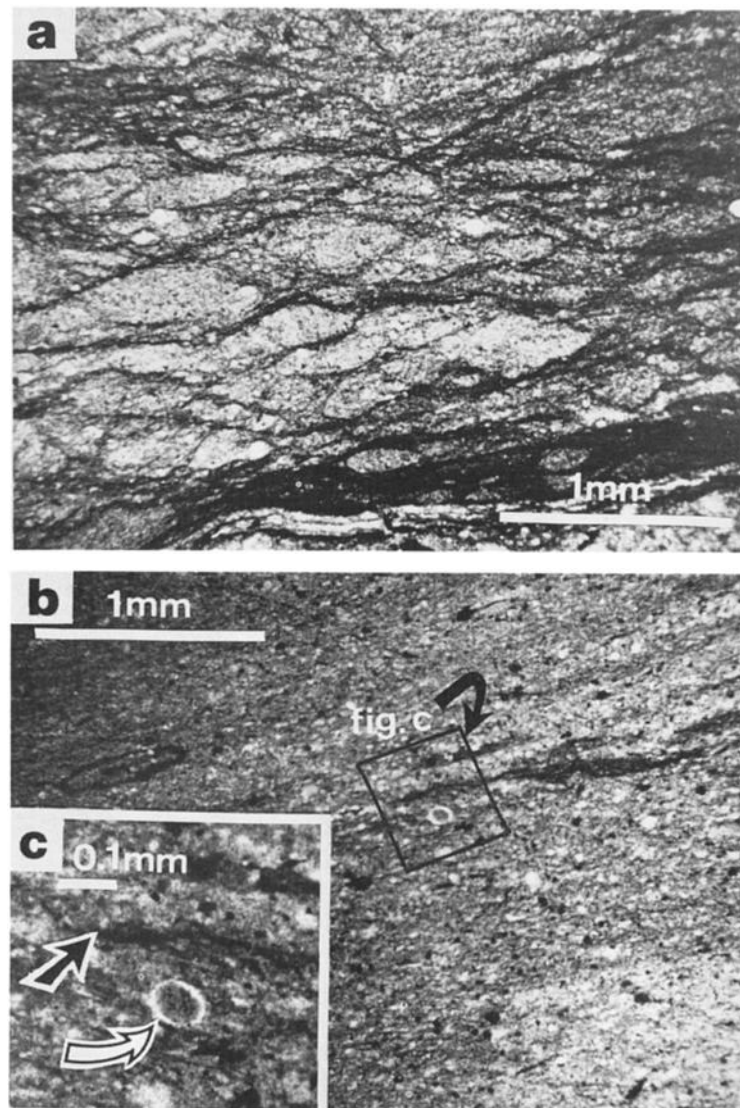


Fig. 14. Microscopic texture of scaly shale of the matrix of the melange. (a) Rhombic domains surrounded by two oriented foliations which merged into each other. This texture indicates the major shear and Riedel shears along the foliation. (b) Primitive foliations developed in the shale of the matrix. Shear zone shown by dark seams are

arranged en echelon. (c) Deformed radiolaria (white arrow) and shear gouge (solid arrow). The long axis of ellipsoidal radiolaria (determined by assuming the original radiolaria is spherical) is oblique to shear planes. This pattern of deformation shows apparently shear along the foliation plane.

parallel shear results from tectonic loading above the decollement, while Needham [1987] and Needham and Mackenzie [1988] suggested a different mechanism for the extension. Namely, they pointed out that the normal faults showing extension parallel to the shear direction are synthetic Riedel shears recognized generally in shear zones [e.g., Platt and Leggett, 1986]. Needham [1987] and

Needham and Mackenzie [1988] also emphasized a different system of veins having a trend perpendicular to the strike of melange and foliation although Byrne [1984] had already reported their development from the Kodiak. This type of veins was formed by layer-parallel extension perpendicular to the shear direction. Needham [1987] and Needham and Mackenzie [1988] interpreted the extension

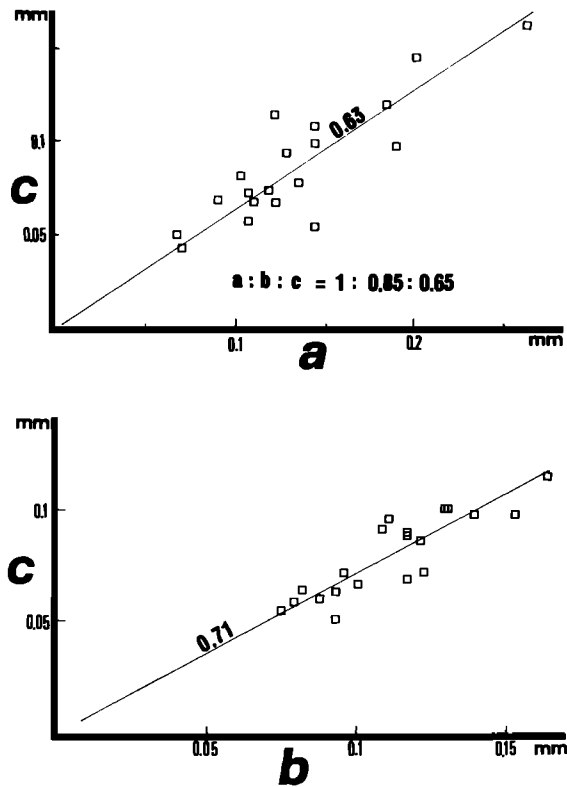


Fig. 15. Deformation of radiolaria. a,b,c means the longest, intermediate and shortest axes of elliptical radiolaria. (a) X-Y plots showing ratios between intermediate and shortest axes in thin sections made perpendicular to the foliation and shear direction. (b) X-Y plots showing the ratio between the longest and shortest axes in thin sections perpendicular to the foliation and parallel to the shear direction.

related to the veins in terms of "sticking thrust model". Our observation shows that layer-parallel extension related to normal faults is earlier than veins and nearly parallel to the shear direction. Although veins filled by calcite and/or quartz are reported to show extension parallel to the shear direction in the Kodiak example [Fisher and Byrne, 1987], our observation in the Shimanto Belt indicates that the dominant orientation of the veins is consistent with a sticking-thrust model. Veins showing extension parallel to the shear direction are observed but not dominant.

The first extension parallel to the shear direction appears to result from Riedel shear as suggested by Needham [1987]. The reason why the Riedel shears are selectively developed without any other structures in association with layer-parallel shear, is attributed to the tectonic loading suggested by

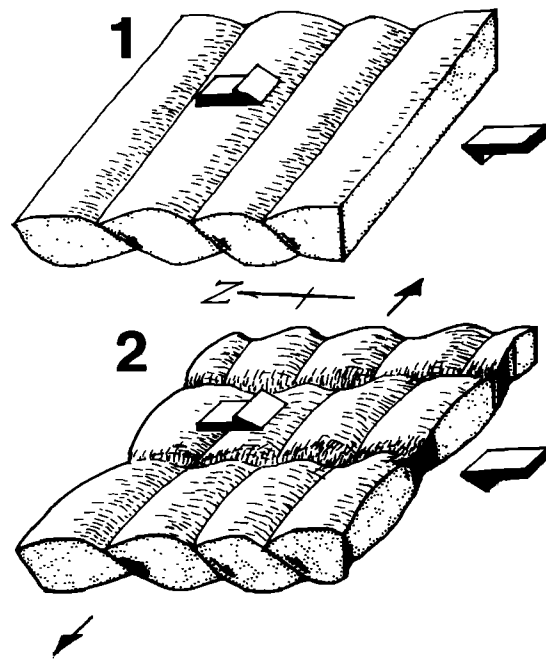


Fig. 16. Generalized picture of shearing and deformation of sandstone in the melange. The N-S trending extension due to normal faults (Riedel shears) in association with layer parallel shearing (1), earlier than E-W trending extension parallel to the strike of layering (2).

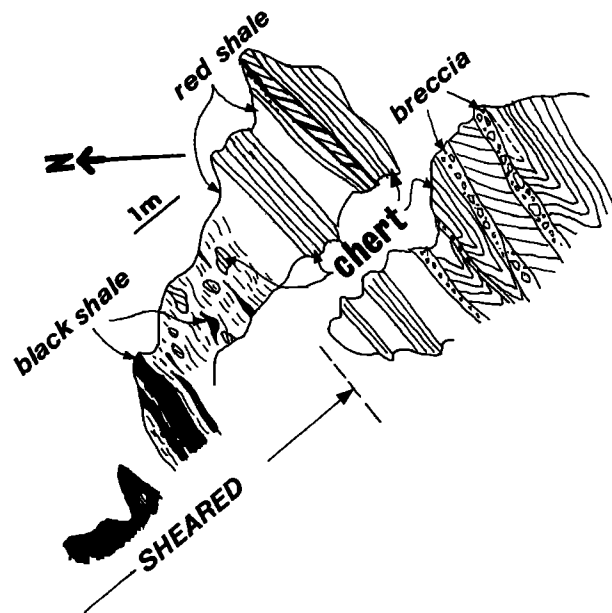


Fig. 17. Mode of occurrence of cherts, red shales and sheared black shales. The pervasive shear zone is recognized near the boundary between the cherts and black shale.

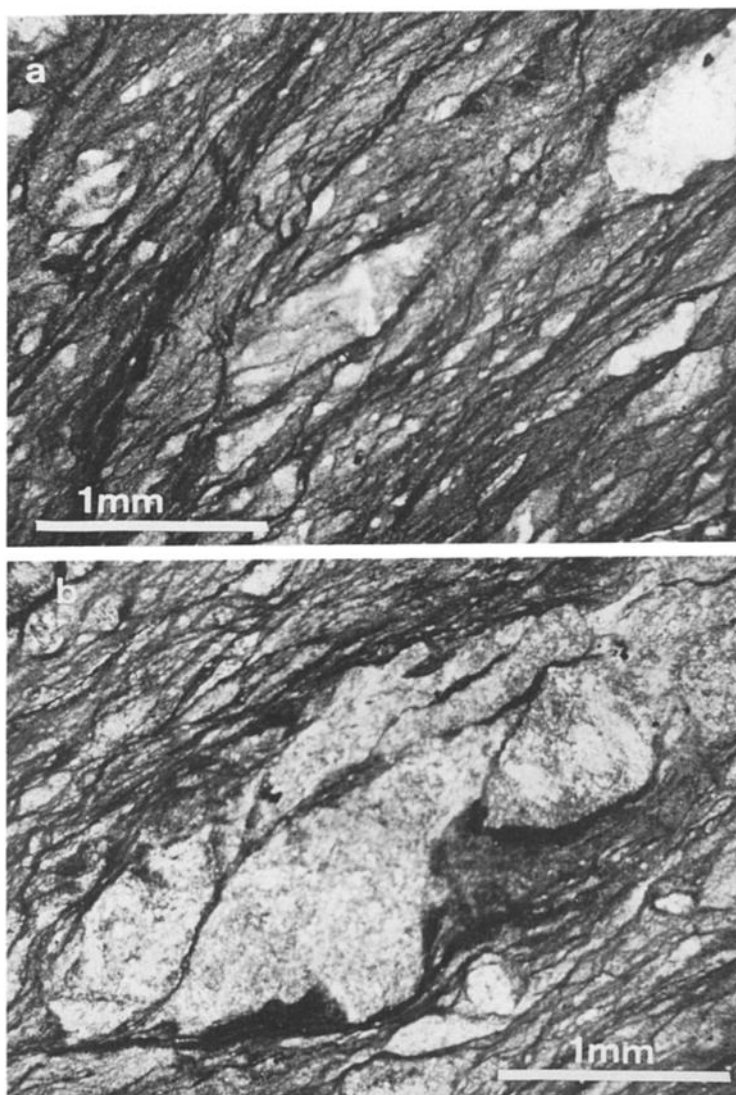


Fig. 18. Features of fine grained chert blocks surrounded by sheared shale matrix under the microscope. (a) Rhombic shaped chert fragments are surrounded by black shale with two orientation fabrics (uncrossed nicols) (b) Broken chert fragments

in the sheared shale. Shale injection along fractures in the chert blocks is recognized (crossed nicols). Note that the fracture pattern of chert blocks is rhombic.

Fisher and Byrne [1987]. As a result, the first extension is regarded as flattening due to simple shear plus pure shear. The second extension perpendicular to the first one is interpreted as due to the sticking-thrust model, because the extension due to sticking thrust is more likely after some quantity of displacement along the thrust.

Strain of melange and shape of lenses. The reason why the longest axis of lenticular sandstone is perpendicular to the stretching direction of melange is considered as follows. Generally, the spacing of

extension fractures normal to the layering is controlled by the thickness of the layer and the lithofacies. Classic studies such as Anderson [1951] and Price [1959] pointed out that the spacing is intimately related to the strength of rocks, which means the ability to store strain energy. Extension fractures due to layer-parallel extension in stronger rocks have a spacing larger than those in weaker rocks in the case of the same thickness of layers but different lithofacies. In this study, the spacing of extension fractures within the sandstone layers

depends mainly on the spacing of normal faults in the shear direction, while the spacing in the direction perpendicular to the shear direction is similar to that of vein fractures (Figure 16). As the normal faults were formed earlier than veins, sandstones during normal faulting seem to have been more loosely consolidated than those at the time of vein formation as discussed previously. The change of consolidation between the time of normal faulting and vein formation might control the spacing of extension fractures. The strength of the sandstone during vein formation seems to be larger than that of the earlier sandstone during normal faulting because of the difference of consolidation. The stronger sandstone has a larger spacing of faults than the weaker one. Consequently, sandstone layers having the same thickness show different spacings in different stages of extension and lenticular sandstone blocks have a long axis perpendicular to the shear direction.

Strain deduced from the deformed radiolaria shows stretching parallel to the shear direction and flattening mostly perpendicular to the layering. Strain of the metamorphosed accretionary complex in Kyushu indicates a prolate type of strain ellipsoid whose longest axis is parallel to the stretching lineation [Toriumi and Teruya, 1988]. The strain ellipsoid in this area is different from that in Kyushu as flattening is apparent. This difference is probably due to a difference of deformation grade. The Shimanto complex showing greenschist facies metamorphism in Kyushu was buried deeper than the rocks in the study area. Strain patterns of the melange in this area suggest that at shallower level of the accretionary complex, a flattening effect is apparent together with stretching associated with layer-parallel shear.

Mixing Process of Oceanic Materials With Terrigenous Sediments (Melange II) and Underplating

As well as Melange I, Melange II is composed of blocks of oceanic materials in the terrigenous shale matrix, and it may be of tectonic origin. Melange II occurs only near the boundary between Melange I and slabs of oceanic materials. Oceanic materials such as cherts become smaller due to shearing, which is the same mechanism responsible for breaking sandstone lenses in Melange I as mentioned above.

In the Akamatsu River, basalt and chert units alternate with Melange I, composed of sandstone blocks in scaly shale matrix. The geologic structure along the Akamatsu River indicates repetition of

Melange I and oceanic units due to imbricated thrusts. How were these occurrences and structures formed? We consider that they show progressive deformation of underthrusting sediments and final underplating underneath the accretionary prism. Figure 19 shows a simplified model of melange pile in the Akamatsu River. As suggested by Fisher and Byrne [1987], Needham [1987], Mackenzie et al. [1987] and Needham and Mackenzie [1988], the melange that originated from trench fill turbidites (Melange I in this study) may be formed by shear in association with underthrusting near decollement. First, the deformation starts near the deformation front. As the sediments are not consolidated, they become harder after deformation and shearing due to strain hardening [Knipe, 1986, Knipe and Needham, 1986; Moore et al., 1987; Moore and Byrne, 1987]. The deformation in the shear zone moves toward the deeper position of underthrust sediments, and the previous shear zone in the upper horizon is abandoned due to hardening [Moore and Byrne, 1987]. This migration means expansion of the shear zone and migration of decollement to a deeper level. Two stages of extension show progressive deformation of the underthrusting sediments. The trench fill sediments deeper than those just beneath the decollement are deformed later because they are incorporated into the shear zone later. When the shear zone migrates and reaches the base of terrigenous sediments, a thick pile of Melange I was formed and the decollement would penetrate the pelagic sediments and basement rocks. At this time, Melange II is formed by shearing (Figure 19).

In the study area, the melange pile with oceanic units at its bottom is about 500m in thickness. This sequence forms a unit between the first decollement and basement rocks. Subsequently, underplating takes place and a duplex pile is created underneath the accretionary prism as suggested by many previous workers [Silver, et al., 1985; Sample and Fisher, 1986; Byrne, 1984]. The final stage of deformation in Melange I shows compression with layer-parallel shear. This is probably related to compression just before or during thrusting in association with underplating (Figure 19). The deformation mode of melange and imbricated stacks of melanges with oceanic materials are consistent with the underplating mechanism of this model. In the melange complex of the Shimanto Belt, however, there are some differences from a general model for underplated material. Although an underplating process has been considered to take place at a great depth where greenschist facies metamorphism occurs [Needham and Mackenzie, 1988; Mackenzie et al., 1987; Fisher and Bryne, 1987], the occurrence of

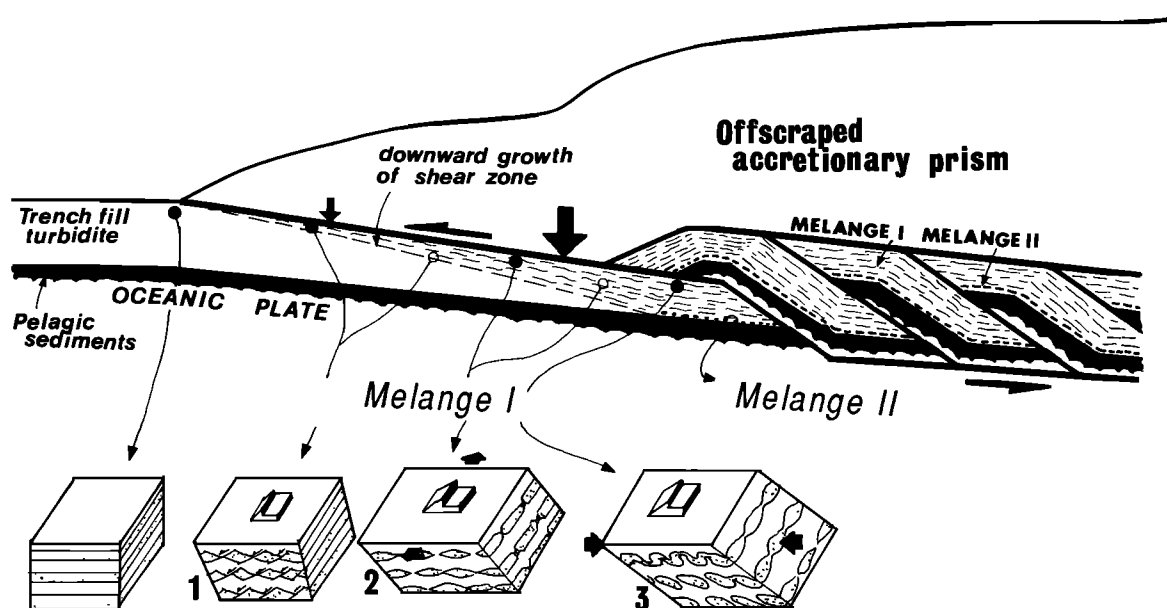


Fig. 19. A model of melange formation and subsequent underplating. Shear zone due to decollement grows downward during the underthrusting of trench-fill sediments. Melange I is formed progressively in association with downward growth of the shear zone. Deeper parts of the trench-fill sediments are deformed later than the sediment in the shallower parts. When the shear zone reaches the base of the trench-fill sediments, a thick section of Melange I is formed. Melange I becomes thinner

as it enters into deeper horizons due to pore reduction and flattening. Subsequently, the shear zone penetrates pelagic sediments and the oceanic basement and Melange II is formed by shearing at the boundary between Melange I and underlying oceanic materials. The section of Melange I with parts of oceanic materials in its base is underplated through duplex formation beneath off-scraped accretionary prism as suggested by Silver et al. [1985].

melange in the Shimanto Belt in eastern Shikoku suggests that the underplating occurs at a shallower depth than previously considered. Metamorphism is not as high as greenschist facies and strain in the shale matrix is less than in metamorphosed terranes in the Shimanto Belt of Kyushu. Fisher and Bryne [1987] suggested that there are coherent trench-fill sediments between oceanic basement and the melange showing the shear zone of the decollement in the Kodiak example, whereas there are no coherent sediments between Melange I and oceanic materials in this area of Shimanto. As pointed out by Moore and Silver [1987], the depth of underplating of oceanic sediments and basement rocks depends on the quantity of sediment supplied into the trench. A thick trench fill introduces sediment subduction and no underplating of oceanic materials occurs, whereas a small quantity of trench fill triggers underplating of oceanic materials. In the case of the Shimanto Belt, the thickness of the shear zone represented by melange is about 500m and oceanic material under the melange appears to have been underplated. This

example gives one of the keys to clarifying the mechanisms of underplating.

Acknowledgments. We are grateful to T. Beku, M. Mukai and M. Kasai for their support of our field and laboratory work. We express sincere thanks to A. Taira, T. Ashi, T. Uemura, and K. Kimura for their valuable suggestions. The earlier draft was reviewed by Y. Ogawa for whom we are grateful. J. C. Moore, D. Cowan and S. Maruyama reviewed our paper and gave us very useful suggestions, which we also appreciate very much.

REFERENCES

- Aalto, K.R., Multistage melange in the Franciscan complex, northernmost California, *Geology*, 9, 602-607, 1981.
- Agar, S. M., Shearing of partially consolidated sediments in a lower trench slope setting, Shimanto Belt, SW Japan, *J. Struct. Geol.* 10, 21-32, 1988.

- Anderson, E.M., *The Dynamics of faulting*, Oliver and Boyd, Edinburgh, 206p. 1951.
- Aoki, Y., T. Tamano, and T. S. Kato, Detailed structure of the Nankai trough from migrated seismic sections, in *Studies in Continental Margin Geology, Mem. 34*, edited by J. S. Watkins and C. L. Drake, pp. 309-324, American Association of Petroleum Geologists, Tulsa, Okla., 1982.
- Biju-Duval, B., P. Le Quellec, A. Mascle, V. Renard, and P. Valery, Multibeam bathymetric survey and high resolution seismic investigations of the Barbados Ridge complex (Eastern Caribbean): A key to the knowledge and interpretation of an accretionary wedge, *Tectonophysics*, *86*, 275-304, 1982.
- Byrne, T., Early deformation in melange Terranes of the Ghost Rocks Formation, Kodiak Islands, Alaska, *Spec. Pap. Geol. Soc. Am.*, *198*, 21-51, 1984.
- Cowan, D. S., Deformation of partly dewatered and consolidated Franciscan sediments near Piedras Blancas Point, CA, in *Trench and Forearc Sedimentation and Tectonics, Spec. Publ. 10* edited by J. Leggett, pp. 439-457, Geological Society of London, 1982.
- Cowan, D. S., Structural styles in Mesozoic and Cenozoic melanges in the western Cordillera of North America, *Geol. Soc. Am. Bull.*, *96*, 451-462, 1985.
- Fisher, D., and T. Byrne, Structural evolution of underthrust sediments, Kodiak Islands Alaska, *Tectonics*, *6*, 775-793, 1987.
- Knipe, R. J., Deformation mechanism path diagrams, in *Structural Fabrics in Deep Sea Drilling Project Cores From Forearcs, Mem. 166*, edited by J. C. Moore, pp. 151-159, Geological Society of America, Boulder, Colo., 1986.
- Knipe, R. J., and D. T. Needham, Deformation process in accretionary wedges- examples from the SW margin of the Southern Uplands, Scotland, *Collision Tectonics, Spec. Publ. 19*, edited by M.P. Coward and A.C. Ries, pp. 51-65, 1986.
- Kumon, F., Coarse clastic rocks of the Shimanto Supergroup in Eastern Shikoku and Kii Peninsula, Southwest Japan, *Mem. Fac. Sci., Kyoto Univ., Seri. Geol. Mineral.*, *50*, 63-109, 1983.
- Lundberg, N., and J. C. Moore, Macroscopic structural features in Deep Sea Drilling Project cores from forearc regions, in *Structural Fabrics in Deep Sea Drilling Project Cores From Forearcs, Mem. 166*, edited by J. C. Moore, pp. 13-44, Geological Society of America, Boulder, Colo., 1986.
- Mackenzie, J. S., D. T. Needham, and S. M. Agar, Progressive deformation in an accretionary complex: an example from the Shimanto Belt of eastern Kyushu, southwest Japan, *Geology*, *15*, 353-356, 1987.
- Matsugi, H., H. Yasuda, S. Okamura, Geologic process of Lower Cretaceous Shimanto Belt, Shikoku (Abstract) *Annu. Meeting, Geol. Soc. Japan, 94th*, 116, 1987.
- McCarthy, J., and D. Scholl, Mechanisms of subduction accretion along the central Aleutian Trench, *Geol. Soc. Am. Bull.*, *96*, 691-701, 1985.
- Moore, J. C., and T. Byrne, Thickening of fault zones: A mechanism of melange formation in accreting sediments, *Geology*, *15*, 1040-1043, 1987.
- Moore, J. C., and E. A. Silver, Continental margin tectonics: submarine accretionary prisms, *Rev. Geophys.*, *25*, 1305-1312, 1987.
- Moore, J. C., S. Roeske, N. Lundberg, J. Schoonmker, D. Cowan, E. Gonzales, and S. Lucas, Scaly fabrics from Deep Sea Drilling Project cores from forearcs, in *Structural Fabrics in Deep Sea Drilling Project Cores from Forearcs, Mem. 166*, edited by J.C. Moore, pp. 55-73, Geological Society of America, Boulder, Colo., 1987.
- Needham, D.T., Asymmetric extensional structures and their implication for the generation of melanges, *Geol. Mag.*, *124*, 311-318, 1987.
- Needham, D. T., and J. S. Mackenzie, Structural evolution of the Shimanto Belt accretionary complex in the area of the Gokase River, Kyushu, SW Japan, *J. Geol. Soc., London.*, *145*, 85-94, 1988.
- Ogawa, Y., K. Hisada, and K. Sashida, Shimanto Supergroup in the Kanto Mountains-A review, *Mod. Geol.*, *12*, 127-146, 1988.
- Pickerings, K.T., S.M. Agar, and Y. Ogawa, Genesis and deformation of mud injections containing chaotic basalt- limestone-chert associations: Examples from the southwest Japan forearc, *Geology*, *16*, 881-885, 1988.
- Platt, J.P. and J.K. Leggett, Structural extension in thrust footwalls, Makran accretionary prism: Implications for thrust tectonics, *Am. Assoc. Petr. Geol. Bull.*, *70*, 191-203, 1986.
- Price, N.J., Mechanics of jointing in rocks, *Geol. Soc. Am. Bull.*, *53*, 381-407, 1959.
- Raymond, L. A., Classification of melanges, *Spec. Pap. Geol. Soc. Am.*, *198*, 7-20, 1984.
- Sakai, T., and K. Kanmera, Stratigraphy of the Shimanto terrain and tectono-stratigraphic setting of greenstones in the northern part of Miyazaki Prefecture Kyushu, Japan, *Kyushu Univ. Sci. Rep., Dept. Geol.*, *19*, 31-48, 1981.
- Sample, J. C., and D. M. Fisher, Duplex accretion and underplating in an ancient accretionary complex, Kodiak Islands, Alaska, *Geology*, *14*, 160-163, 1986.

- Silver, E. A., M. J. Ellis, N. A. Breen, T. H. Shipley, Comments on the growth of accretionary wedges, *Geology*, 13, 6-9, 1985.
- Suyari, K., Restudy of the Northern Shimanto Subbelt in Eastern Shikoku, *J. Sci., Univ. Tokushima*, 19, 45-54, 1986.
- Taira, A., Sedimentary evolution of the Shikoku subduction zone: Shimanto and Nankai Trough. in *Formation of Ocean Margins*, edited by N.Nasu, K.Kobayashi, S.Uyeda, I.Kushino, and H.Kagami, pp.835-851, Terra Scientific Publishing Company, Tokyo, 1985.
- Taira, A., M. Tashiro, M. Okamura, and J. Katto, The geology of the Shimanto Belt in Kochi Prefecture, Shikoku, Japan, in *Geology and Papers in Honor of Prof. J. Katto*, edited by A. Taira and M. Tashiro, pp.319-389, Rinyakosaikai Press, Kochi, Japan, 1980.
- Taira, A., J. Katto, M. Tashiro, M. Okamura, and K. Kodama, The Shimanto Belt in Shikoku, Japan- Evolution of Cretaceous to Miocene accretionary prism, *Mod. Geol.*, 12, 3-46, 1988.
- Toriumi, M. and J. Teruya, Tectono-metamorphism of the Shimanto Belt. *Mod. Geol.*, 12, 303-324, 1988.
- Uemura, T., Tectonic analysis of the boudin structure in the Muro group, Kii peninsula, southwest Japan, *J. Earth Sci. Nagoya Univ.*, 13, 99-114, 1965.
- Westbrook, G., A. Mascle, and B. Biji-Duval, Geophysics and structure of the Lesser Antilles forearc, in *Initial Reports of the Deep Sea Drilling Project, 78* edited by B.Biji-Duval et. al., pp23-38, U. S. Government Printing Office, Washington, D.C., 1984.
-
- G.Kimura and A.Mukai, Department of Earth Sciences, Faculty of Education, Kagawa University, Takamatu, Kagawa, 760 Japan.

(Received March 22, 1989;
revised March 26, 1990;
accepted April 4, 1990.)